Meteor head velocity determination

G. Stober, Ch. Jacobi

March 29, 2007

Zusammenfassung

Meteore, die in die Atmosphäre eindringen, bilden bei hohen Oberflächentemperaturen, die durch Kollisionen mit der umgebenden Luft hervorgerufen werden, einen mehrere Kilometer langen Plasmaschweif aus. An diesem Schweif werden ausgesandte Radarwellen reflektiert und zurückgestreut. Dies führt zu einem charakteristischen Schwingungsverhalten, auch Fresnel Zonen genannt, am Empfänger. Die Überlagerung dieser Wellen ist verantwortlich für die typische Signalform eines Meteors, mit dem abrupten Anstieg und dem exponentiellen Abfall für "underdense" Meteore. Mit Hilfe einer Simulation wird der theoretische Zusammenhang zwischen Geschwindigkeit und Signalverlauf demonstriert. Des weiteren wird gezeigt, das die Methode von Baggaley et al. [1997] zur Bestimmung von Meteoreintrittsgeschwindigkeiten auch auf ein Radarinterferometer (SKiYMET) anwendbar ist. Abschliessend werden die gewonnen Ergebnisse mit einem anderen Verfahren sowie der Literatur verglichen.

Abstract

Meteors, penetrating the earths atmosphere, creating at high surface temperatures, which are caused by collisions with the surrounding air molecules, a several kilometer long plasma trail. The ionized plasma backscatters transmitted radar waves. This leads to characteristic oscillations, called Fresnel zones, at the receiver. The interference of these waves entails the typical signal shape of a underdense meteor with the sudden rise of the signal and the exponential decay. By means of a simulation the theoretical connection between velocity and signal shape is demonstrated. Furthermore it is presented, that the method from Baggaley et al.[1997] for determination of meteor entry velocities is applicable for a radar interferometer (SKiYMET). Finally the results are compared to other radar methods on similar equipment and to other experiments.

1 Introduction

As meteoroids enter the earth's atmosphere they form a cylindrical plasma trail. This trail is detected by the SKiYMET backscatter meteor radar at Collm observatory (51.3° N, 13° E). Previous articles already described the use of the meteoric ionization to determine a mesopause temperature from the ambipolar diffusion coefficient, which corresponds to the decay time of the received signal (Hocking et al. [1999,2001,2004] and Stober et al.[2006]). It's also well known that the plasma is drifted due to the prevailing winds in the meteor layer, resulting in a radial velocity component of the meteor echo. All the necessary parameters (e.g. radial velocity, theta, phi, τ, etc) for the calculation of these meteorological information are obtained by automatic computer routines for the signal analysis. A more detailed description is given in Hocking et al. [2001] and Stober [2006].
A meteor head velocity measurement is non-standard for the SKiYMET radar, operated at Leipzig University. Therefore, the first step was to create a model of a meteor entering the atmosphere. The numerical simulation includes all important parameters the echo depend on, such as the range R, the PRF (Pulse Repetition Frequency), the meteor head velocity v (simulation velocity), the decay time (τ), the transmitting power P_T, the antenna gains for the transmitter, the receiver G_T and G_R and finally the electron line density q.
With this simulation it was possible to implement the method of Baggaley [1997], who used the rising time of signal, which consists of several successive Fresnel zones close to the specular point of the meteor echo. Other methods are the pre-t_0 or post-t_0 approach, which work as well as the rising time method in

theory, but often the signal power is too weak, especially in the early stages of the signal pre-t_0 that it is very difficult to separate the white noise of the amplifier from a real signal. This makes an application of this procedure very difficult by a computer analysis program. On the ofter hand the post-t_0 method suffers from the problem of prevailing winds and the ambipolar diffusion. Both processes have to be removed, before the signal could be analyzed. In practice this removal is often not possible. Of course the pre-t_0 and the post-t_0 approach have shown, that if the data (1-3%) can be analyzed, that they have a slightly higher accuracy than the rising time method.
Determining meteor head velocities may provide valuable information, especially the possible distinguishing of space debris from real meteor is of interest. Other studies showed that with the knowledge of the meteor speed and implementing meteor models the mass, the mass ablation and the atmospheric density can be estimated (Hunt et al. [2003]).

2 Meteoric plasma production

A meteor traveling with velocities between 12-72 km/s through the atmosphere is heated up by colliding with the air molecules. When the surface of the meteoroid reaches a temperature of about 1850 K (Baggaley [2002]) the mass ablation process starts. Hence the mass ablation starts in an altitude of 70-100 km. The typical impacting species are O_2 and N_2. Since the ionization potentials of O_2 and N_2 are higher than those of the meteoric constituents Ca, Fe, Mg, Si and Na the plasma trail includes mainly metallic ions. For the operation of the radar sampling the number of free electrons is more important. Assuming an ambipolar process in the plasma the ionic and the electronic component have a common dynamic behavior (Prölss [2004], Stober [2006]). The following empirical formula connects the free electron density q with the velocity v, the effective ionization parameter β and the meteoric mass of the ablated atoms μ;

$$q \;=\; -\frac{\beta}{\mu v}\frac{dm}{dt} \tag{1}$$

The effective ionization is described by the Jones model 1997;

$$\beta \;=\; 9.4 \cdot 10^{-6}(v - v_{threshold})^2 V^{0.8} \quad . \tag{2}$$

3 Meteor echo formation process

The geometry of our experiment is very important. In the case of a backscatter radar the strongest signal is received, when the meteor is passing the specular condition. That means the point where the meteor velocity vector is perpendicular to the radar radiant vector. This part of the signal is further on the time reference and called the t_0-oscillation. Of course like in every other scattering process there is also some energy reflected before passing through the specular condition. This reflection shows typical Fresnel zones which can be used for velocity determination. These oscillation are more than 1000 times weaker than the t_0 signal of the meteor and known as pre-t_0 oscillations or Fresnel zones. Thus, this method is very susceptible to bad signal to noise ratios.
Studying the time behavior of the electric field at our receiver will give us a better understanding of the echo formation process. The electric field is proportional to the term;

$$E\ ds \;\propto\; q\ exp\left(i\left(\omega t - \frac{4\pi R}{\lambda}\right)\right) ds \quad , \tag{3}$$

where q is the electron density (1), R the radial distance, λ the radar wavelength and ω the angular frequency. Therefore the total electric field received by the plasma trail is given by the integral along the track length;

$$E \;\propto\; q\int_0^s sin\left(\omega t - \frac{4\pi R}{\lambda}\right) ds \quad . \tag{4}$$

Assuming q as constant along the trail and integrating along the trail length s will give the total electric field at the antennas. Take into account the geometry and simplifying the slowly changing range near to the orthogonality position the total electric field can be expressed in terms of the Fresnel integrals;

$$E \propto q(C\ sin\chi - S\ cos\chi) \quad and \quad \chi = \left(\omega t - \frac{4\pi R}{\lambda}\right) \quad , \tag{5}$$

with

$$C = \int_{-\infty}^{x} cos\left(\frac{\pi x^2}{2}\right) dx \quad and \quad S = \int_{-\infty}^{x} sin\left(\frac{\pi x^2}{2}\right) \quad . \tag{6}$$

This leads to the backscattered power at the radar antennas;

$$P_R = \frac{P_T G_T G_R \lambda^3 \sigma_e}{128\pi^3 R^3} q^2 \left(\frac{C^2 + S^2}{2}\right) \quad . \tag{7}$$

4 Numerical simulation of the meteor echo formation

The numerical simulation of the meteor echo formation process is based on the Fresnel integrals. Thus, the numerical solution of these integrals is the main problem. A good illustration of the Fresnel parameters is given by the Cornu Spiral (Fig. 1). There, the relative amplitude is given by a vector from $C = -0.5$ and $S = -0.5$, corresponding to $x = -\infty$ and a point along the curve (Baggaley [2002]), which can be expressed as length of the plasma trail in the atmosphere. Using this information it is possible to separate the received power at the antennas in two parts, the in-phase component C and the quadrature component S. The phase behavior of the two components is given by $tan\phi = (S/C)$.

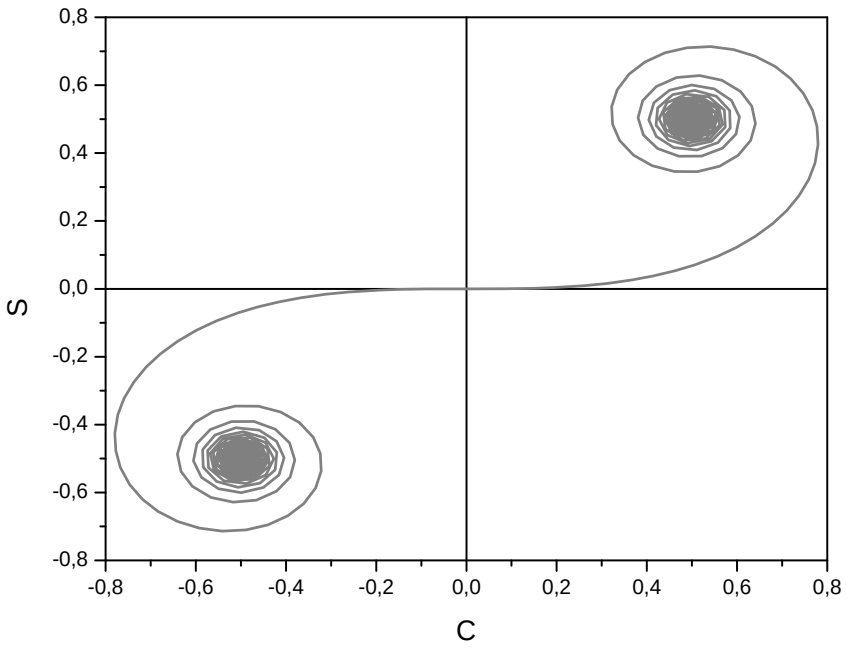

Figure 1: Cornu Spiral illustrates the behavior of the signal received from Fresnel zone. The (0,0) coordinate shows the specular condition.

The final step for simulation is the connection of the Fresnel zone x with time. Assuming a meteor entering the earths atmosphere with velocity v, at a distance R_0 (radial distance at specular point) and

a decay time τ allows to calculate for several time steps the position relative to the radar. The time steps are determined by the PRF (Pulse Repetition Frequency) of the radar. The SKiYMET radar at Collm Observatory uses a 2144 Hz PRF with a 4-time coherent integration, which results in an effective PRF of 536 Hz (Hocking [2000]). Considering all these facts, the angular change in position and range of the meteor is calculated and from that the Fresnel parameter x is deduced. Solving the integrals (6) for the given value of x leads directly to the backscattered power at the antenna. The resulting power can be plotted as time series as well as in the Fresnel parameter x. To simplify the simulation any angular difference of the antenna gains is neglected. This does no damage at all, because the simulation of the time behavior of the signal should be independent from the antennas used at the ground station and from their characteristics. In Figure 2 there are given some typical Fresnel oscillations for different decay times.

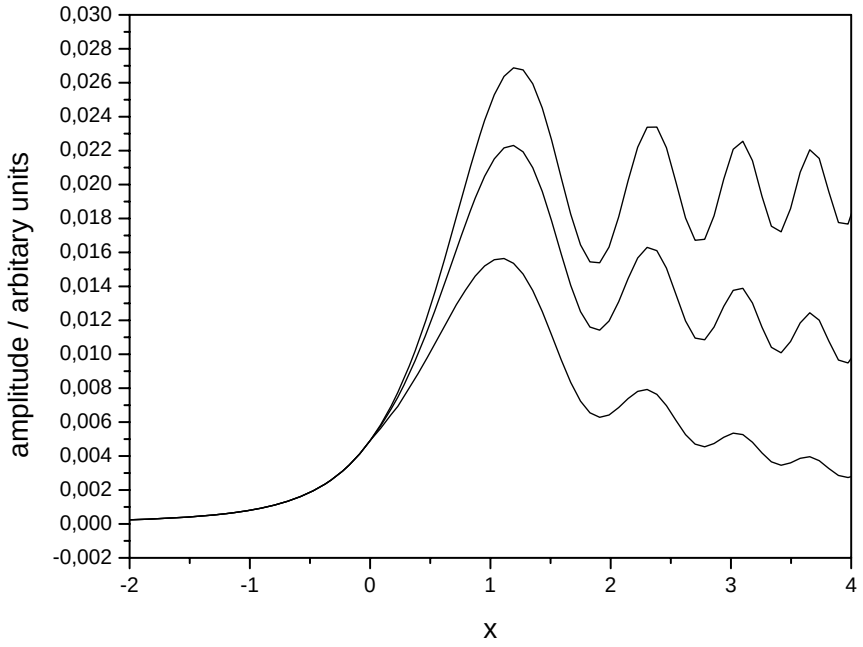

Figure 2: Fresnel oscillation of a specular meteor for different decay times for $\tau = \infty, 0.3, 0.1$ plotted in Fresnel zones.

5 Velocity determination from echo profile measurements

This method was introduced by Baggaley et al. [1997] and uses the Fresnel zones close to the specular condition. The length s of a Fresnel zone is given by the term;

$$s = \frac{\sqrt{R\lambda}}{2}\, x \quad . \tag{8}$$

Therefore the meteor velocity is given as;

$$v = \frac{\sqrt{R\lambda}}{2}\, \frac{dx}{dt} \quad . \tag{9}$$

Note that the maximum resultant amplitude of the standard diffraction as $A_{max} = 1.657$ at $x = 1.217$ and the maximum gradient dA/dx at $x = 0.572$, which correspond to the tangent point in the Cornu

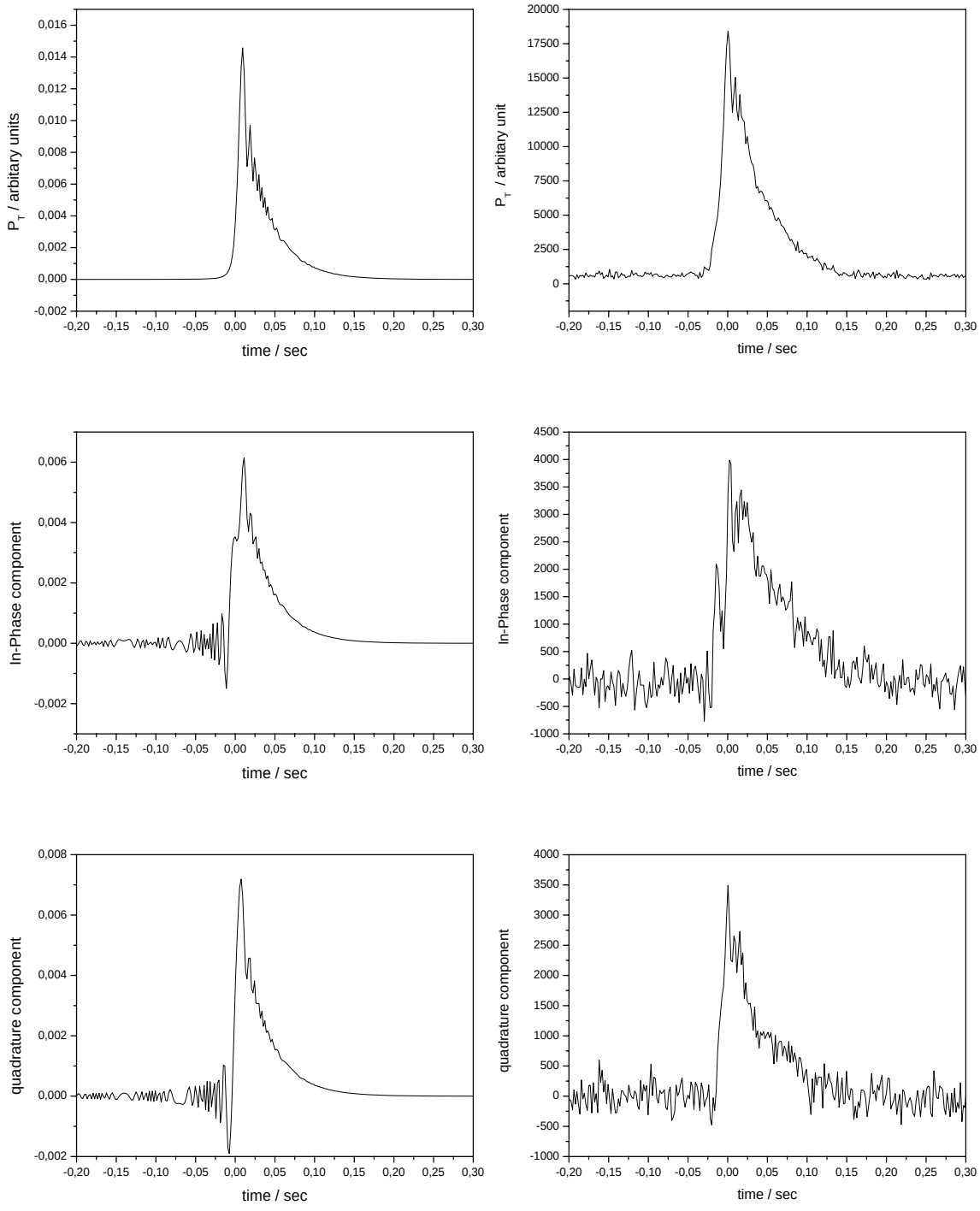

Figure 3: Simulated signal (left) and real signal (right) of a specular meteor echo plotted with a PRF of 536, at a range of 134km and $\tau = 0.034s$ for the amplitude, the in-phase and quadarture components. The simulated signal power is normalized to P_T,G_T and G_R=1.

Spiral. For a radar sampling amplitudes with a PRF Eq. (9) must be slightly modified, which results in;

$$v \;=\; \frac{1.657\ PRF\ \sqrt{R\lambda}}{2\ A_{max}} \left[\frac{\Delta A}{\Delta n}\right]_{max} \quad , \tag{10}$$

for the velocity. The limits of this method are easy to guess. The problem in reality is to find the derivation of the received echo power, especially white noise of the receivers can do severe damage to the data.

Baggaley et al. [1997] performed comparisons to other methods, e.g. optical, pre-t_0 and also multi-site measurements. The investigation delivered a systematic error of -0.6 km/s and a standard deviation of 4 km/s to other independent methods.
Running the above described algorithm on the simulated echo profiles confirmed this systematic bias error. In addition, it is possible to define the exact limits of this method for the radar at Collm Observatory. As Figure 4 shows, the analysis is quite unreliable for very low speeds ($\leq$ 10 km/s) and at very high velocities ($\geq$ 55 km/s) for meteors at minor range of approximately 130 km. The higher the distance from the radar, the lower the accuracy gets for slow targets, but the more reliable is the measurement for very fast meteors. The dependence of the error from the distance provides some problems to correct for this bias. Considering the known effects that most meteors are detected at a range close to 130 km and the dependence of the radio magnitude M from the velocity,

$$M \;=\; 36 - 2.5log_{10}q + 2.5log_{10}V \quad [V]\; in\; \frac{km}{s} \;\; ; \tag{11}$$

lets us conclude that the measurement should show the greatest accuracy in the speed range of 10-35 km/s. This result takes into consideration that the maximum flux occurs at a distance of 130 km (Stober [2006]). Hence, most of the meteors should have speeds of 10-35 km/s. Therefore the following linear bias correction is applied to the data, which guarantees the greatest possible accuracy for this velocity range;

$$V_{corrected} \;=\; \frac{1809.1\frac{m}{s} - V_{measured}}{1.101} \;\; . \tag{12}$$

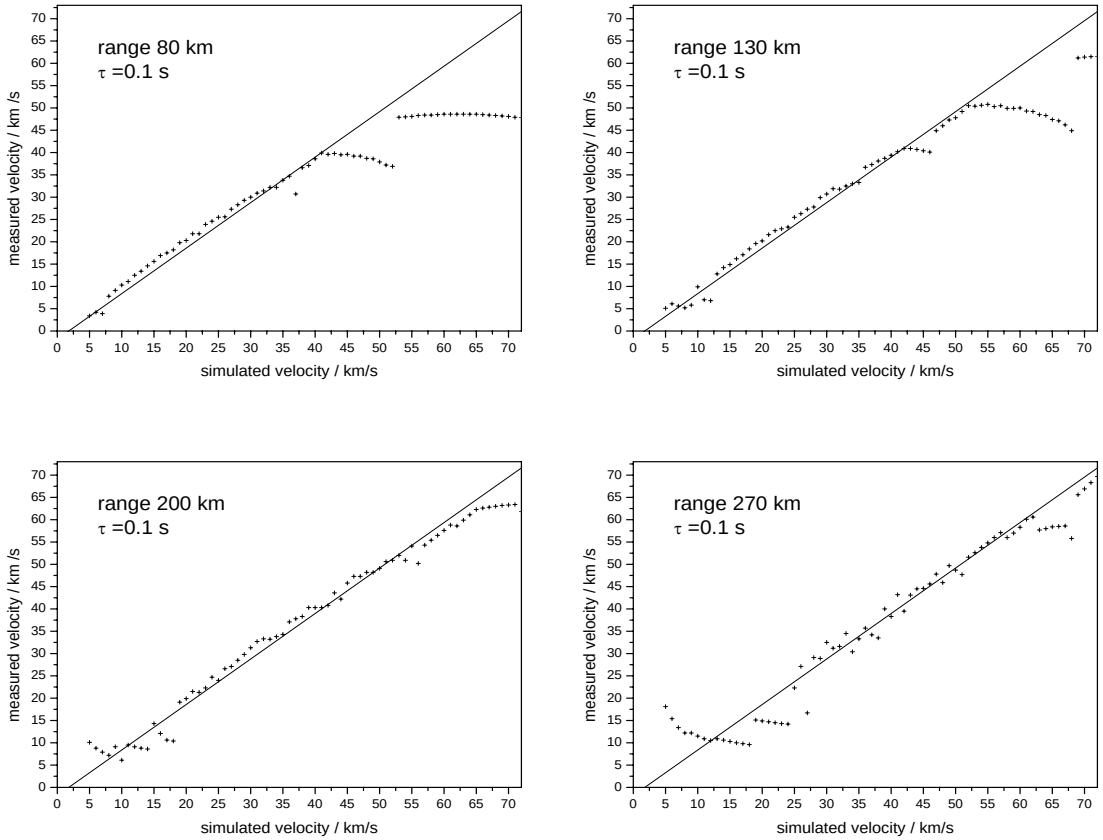

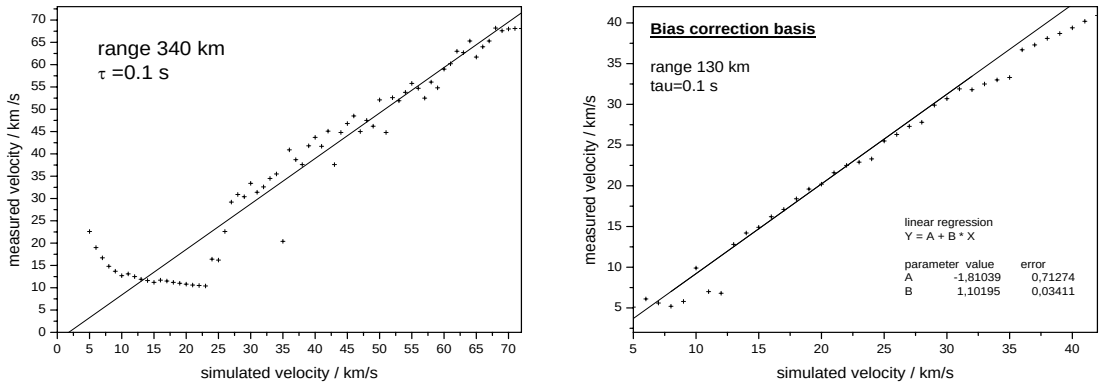

Figure 4: Correlation diagram of the simulated data and the analysis algorithm of the SKiYMET radar operated at Collm with a linear correction fit.

6 Results

Due to disc space limitation no automatic storage of the single receiver data for each meteor event is made. The quadrature and in-phase components from each meteor event are only stored for one month (Hocking et al. [2001]), which means one second of data of the pre-t_0 and three seconds of the post-t_0 signal are stored. We analyzed the Geminids on the December 12-15 and some January data, because on the one hand there is a high count rate of meteors (Geminids) and on the other hand there is data from Kühlungsborn 2006 available. This allows a comparison to a radar using another method at a site close to Collm.

A good basis for a comparison are velocity histograms with 1 km/s bins (Fig. 5). The diagrams show a mean meteor velocity of 17 km/s for both Kühlungsborn and Collm. Remembering the results of the simulation all data below 5 km/s is neglected and as expected from the distance distribution most of the detected meteors are in the range between 10-30 km/s at both sites. Obviously there are some meteor events below 7 km/s, which can be interpreted as space debris. Of course the error for this low speeds is too large to do a more detailed classification. In contrast it is evident that the Kühlungsborn data includes much more of the space debris. But both methods are not able to provide a direct separation of space debris from real meteors events.

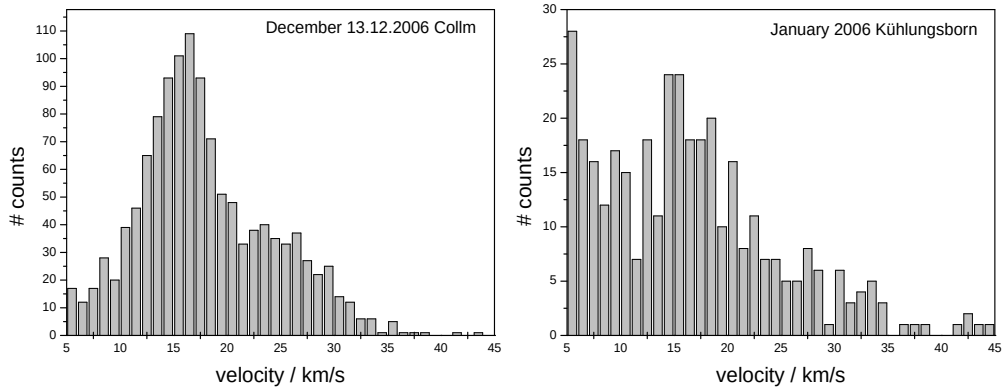

Figure 5: Histograms of the meteor head velocities measured at Collm (left) and Kühlungsborn (right).

A velocity altitude profile indicates a dependence of the velocity on height. It seems that slower meteors tend to ionize at lower altitudes. This effect is also confirmed by optical measurements. But this does

not take into account that always the entry angle of a meteors is related to the specular condition of the radar. This means a steep entry angle is always connected with a large distance to the radar site and shallow angle with a closer distance. Hence meteors with shallow entry angles are detected close to the zenith of the radar site. In addition a shallow entry angle is almost connected with a slower velocity, which means a very fast meteor with an entry angle close to 0° would simply pass the earth without forming a plasma trail or would be reflected from the atmosphere back to space. Only a fast meteor striking the atmosphere at a steep angle can be detected. Both effects are included in Figure 6 and so the large spread around 15 km/s is explainable. At this speed a width spread of possible entry angles exist.

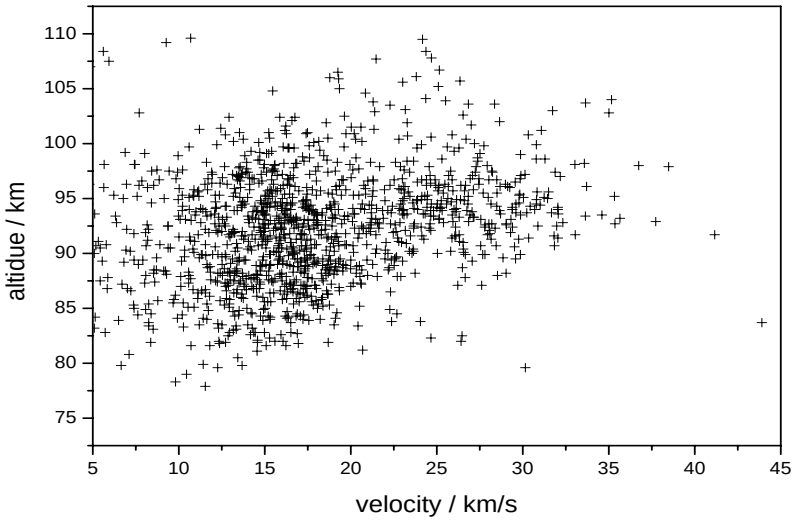

Figure 6: Meteor head speed vs. hight diagram given for the 13.12.2006 during the Geminid shower.

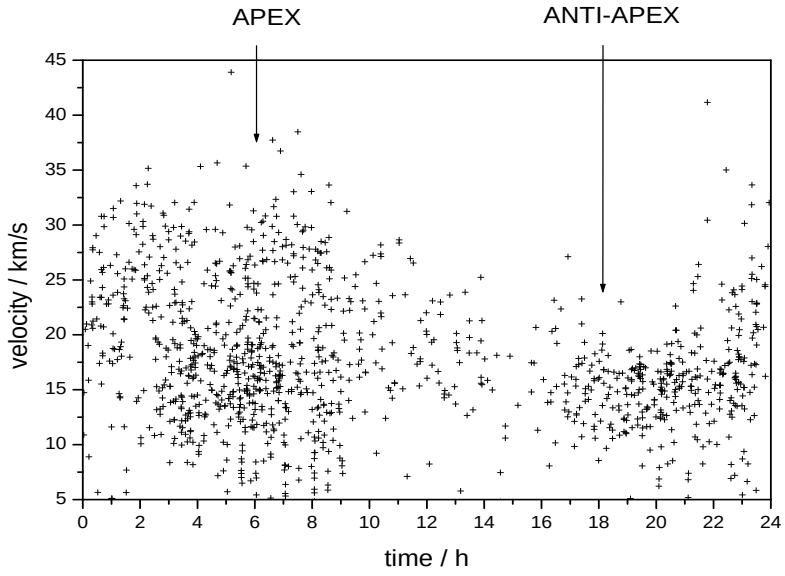

Figure 7: A one day (13.12.2006) profile plot of the meteor velocity indicating the APEX and Anti-APEX. The time is given in UTC.

Finally a graph of time vs. velocity shows the Apex and Anti-Apex of the earth related to the fix star background (Figure 7). Due to the earth rotation the highest velocities are measured during the night,

the lowest at late afternoon. There is one additional fact, that belonging to the meteor flux. Obviously the Anti-Apex point is only the time with lowest meteor head velocities, but not the time of the smallest meteor flux, which is reached two hours earlier. At the moment there is no obvious explanation for this effect.

The results are confirmed by a study in the CMOR (Canadian Meteor Orbit Program) (Webster et al.[2004]). During the work three spaced receivers with distances of several kilometers were used to derive the meteor velocity and flight paths. Hunt et al.[2003] concluded some higher velocities for the meteor entrance speeds using larger radars, designed for astrophysics. The data evaluated there focused on direct head echoes, which were detected with the ATAIR system (9° N, 167°E) and the HRMP (40° N, 270° E). The transmitter power of these systems were in the range of 0.6-4.0 MW.

7 Conclusion

This study illustrates the benefit of the rising time method from Baggaley et al. [1997] as a tool to derive meteor head velocities with a radar interferometer. The good coincidence to other measurements and simulation confirm the accuracy of the algorithm to determine atmospherical meteor speeds. The appliance of this technique provides the ability to study meteor stream velocities as well as other meteor related parameters. The possibility to detect space debris is also outlined.

Acknowledgments

Special thanks go to W. Singer in Kühlungsborn for providing the data, and for the useful discussions. Also the technical support and maintenance of the radar at Collm by D. Kürschner is acknowledged.

References

Baggaley W.J., R.G.T. Bennett, A.D. Taylor, Radar meteor atmospheric speeds determined from echo profile measurements, *Planet. Space Sci., Vol. 45, 5, 577-583*, 1997

Baggaley W.J., 2003: Radar Observations. in: I.P. Williams, E. Murad (Eds.), Meteors in the earth atmosphere, *Cambridge University Press, 123-148*, 2002

Hocking W.K., Thayaparan T. and J. Jones, Meteor decay times and their use in determining a diagnostic mesophereic temperature-pressure parameter: methodology and one year of data, *Geophysical Research Letters, 2977-2980*, 1997

Hocking W.K., Temperatures using radar-meteor decay times,*Geophysical Research Letters, 3297-3300*, 1999

Hocking W.K., Real-time meteor entrance speed determination made with interferometric meteor radars, *Radio Science, Vol. 35, 5, 1205-1220*, 2000

Hocking W.K., B. Fuller, B.Vandepeer, Real-time determination of meteor-related parameters utilizing modern digital technology, *Journal of Atmospheric and Solar-Terrestrial Physics 63*, 2001

Hunt S.M.,M. Oppenheim, S. Close, P.G. Brown, F. McKeen, M. Minardi, Determination of the meteoroid velocity distribution at the Earth using high-gain radar, *Icarus 168, 12, 34-42*, 2003

Prölss G.W., Physik des erdnahen Weltraums. 2. Auflage, *Springer*, 2004

Stober G., Jacobi Ch., Mesopause Temperatures over Collm, *Sci. Rep. Met. Inst. Univ. L. 37, 41-54*, 2006

Stober G., Radar-Temperaturmessung im Mesopausenbereich, *Diploma thesis Met. Inst. Univ. L.*, 2006

Webster A.R:, P.G. Brown, J. Jones, K.J. Ellis, M. Campbell-Brown, Canadian Meteor Orbit Radar (CMOR), *Atmospheric Chemistry and Physics,4,679-684*, 2004